

UDC 549.5.02; 549.27.28

NEW DATA ON VANADIUM HEMATITE ASSOCIATED WITH MICRO- AND NANOCRYSTALS OF NOBLE METALS, COPPER, ZINC, AND IRON MINERALS

Andrey A. Chernikov

Fersman Mineralogical Museum RAS, Moscow, cher@fmm.ru

Victor T. Dubinchuk, Natalia I. Chistyakova, Irena S. Naumova

All-Russian Scientific-Research Institute of Mineral Resources (VIMS), Moscow

Vyacheslav S. Zaitsev

All-Russian Scientific-Research Geological Institute, Saint Petersburg

The dispersed hematite of bed zone of oxidation, isometric aggregations and veinlets of lamellar hematite from ore and the circum-ore space of a fissure deep-seated zone of oxidation contain more than 1% (to 10.96%) of vanadium. It is detected for the first time that vanadium hematite has the characteristic unit cell parameters: $a_{\text{th}} = 5.44 \text{ \AA}$, $\alpha = 54^\circ 73'$; $a_{\text{hex}} = 5.03 \text{ \AA}$, $c = 13.84 \text{ \AA}$, space group R-3c). Vanadium hematite often contains carbonaceous aggregations, on which or near which are powdery aggregates of gold-bearing copper, auricupride, native gold, froodite, isoferroplatinum, intermetal compound CuZn, crystallochemical group of Fe, and a new native phase of the Cu_3Pd type, the palladium analogue of auricupride. Size of nanocrystals of these powdery aggregates varies from 1-5 nm to 300-500 nm. The X-ray characteristic spectra of the Cu_3Pd phase show the visible fluctuations of a ratio of palladium to copper in different particles of this phase, whereas the unit cell parameters of these particles are practically identical, $a_0 = 3.68 \pm 0.03 \text{ \AA}$. The icalculated formulae can be represented as follows: $\text{Cu}_{3.3}\text{Pd}_{0.67}$, $\text{Cu}_{3.3}\text{Pd}_{0.7}$, $\text{Cu}_3\text{Pd}_{1.18}$. A space group of the new phase, Pm3m, is also evidence that it is an analogue of auricupride. In hematized dolomite, a grain of carbonate mineral with diffusive reflections of the $\text{AuO}(\text{OH})$ phase, $a_0 = 4.18 + 0.03 \text{ \AA}$, with sizes of nanocrystals 100-150 nm, was found.

Presence of carbonaceous matter, on which nanocrystals of noble metals and other intermetal compounds grow, is an evidence that analytical data on content of the noble metals in ores and in the zone of hematization of ores can be understated in connection with their evaporation together with carbon during analysis. Therefore, the previous forecasts (Chernikov, 1997, 2001; Chernikov *et al.*, 2000) about large reserves of the noble metals in the region of Onezhskaya depression have one more indirect confirmation.

7 tables, 9 figures, 11 references.

Vanadium hematite is widespread in uranium-vanadium deposits of the Onezhskii type. This type of deposits with noble metals (Pb, Pt, Au, Ag), molybdenum, copper, bismuth etc. is the large ore object on reserves of vanadium and, possibly, accompanying elements, in particular, noble metals. The uranium-vanadium deposits, Srednyaya Padma, Tsarevskoe, Kosmozero etc., are located in the Onezhskaya riftogenetic depression in South Kareliya. The gently dipping disseminated ore bodies of these deposits are confined to grey-colour terrigenous rocks at their contact with red-brown (hematized) dolomites (PR₁) of the old deep-seated bed zone of oxidation (Poluektov *et al.*, 1998; Chernikov, 1997, 2001). From the surface up to a depth of 30 m, rarely 150 m, in all deposits, the near-surface contemporary zone of oxidation occur, in which brown and dark brown oxides of iron and manganese are widespread, they limit uranium-vanadium ores from the top. Moreover, in the ore bodies and in circum-ore space are the isometric aggregations and veinlets of hematite

with dark red – brown to black colour, they are obliged to activity of fissure deep-seated zone of oxidation and cut ore bodies and hematized dolomites. Dolomites with dispersed hematite at the contact with grey-colour rocks, isometric aggregations and veinlets of hematite in ore bodies are enriched by the redeposited noble metals, sometimes uranium; the nature of their separation was not detected by common mineralogical methods. Therefore, a complex of high-precision methods was used: the raster electron microscopy with the X-ray spectrometer and the transmission electron microscopy with microdiffraction analysis, and also the microprobe electron analysis for detection of ultramicroscopic centres of concentration of noble metals, their chemical composition, structure and form of aggregations. Nano- and microcrystals of gold, platinum, palladium, their compounds and uranium oxides in vanadium hematite was studied the most minutely.

This data is important for solution of a number of practical questions, which are considered

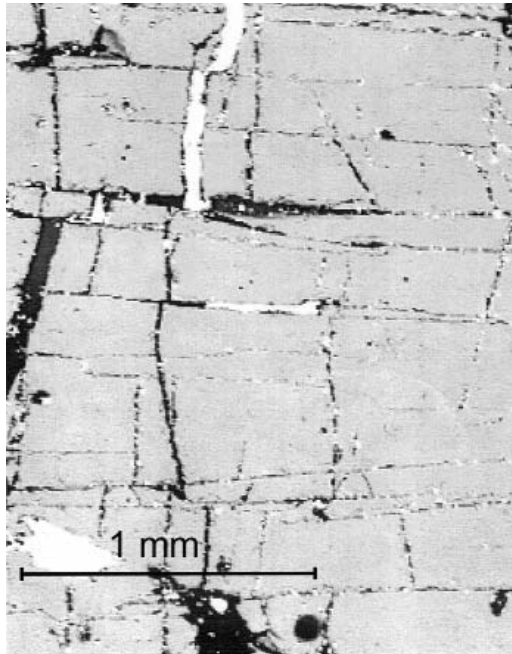


Fig. 1. Lamellae of vanadium hematite (grey), broken in longitudinal and transversal directions by cracks filled up by clausenthalite (light), carbonate (dark grey). Rarely, quartz and clay minerals having the same dark grey colour as carbonate in reflected light crystallize along cracks.

Fig. 2. Lamellae of vanadium hematite with different contrast of image in back-scattered electrons. Lines of hematite with grey contrast contain up to 10.96 % of vanadium; lamellae with light grey contrast contain up to 5 % vanadium. Light aggregations is clausenthalite, black is carbonate.

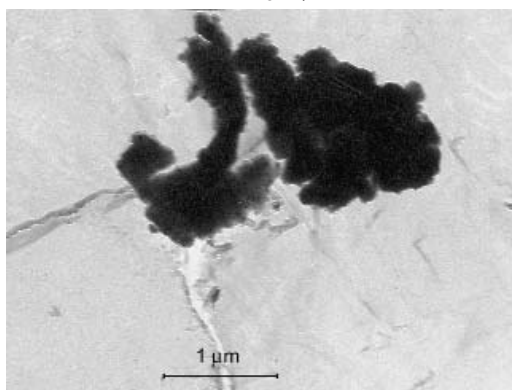
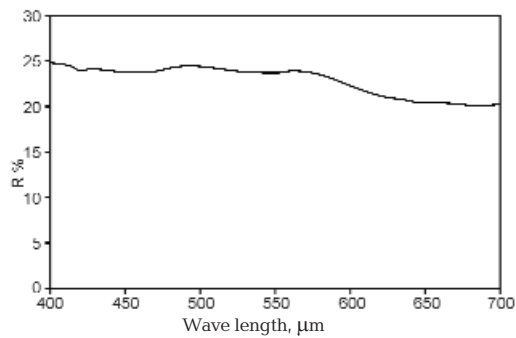
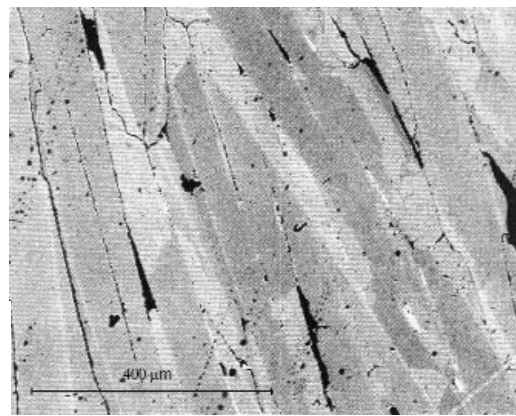


Fig. 3. Refraction coefficient of vanadium hematite.

Fig. 4. Dendrite aggregations of isoferroplatinum, Pt_3Fe .



Fig. 5. Dendrite aggregates of native gold.

Table 1. Chemical composition of vanadium-bearing hematite, %, data of electron microprobe analysis.

| № | Ti | V | Cr | Mn | Fe | Ni | O | Total |
|----|------|-------|------|------|-------|------|-------|--------|
| 1 | 0.53 | 5.21 | 0.06 | 0.04 | 68.48 | 0.04 | 24.11 | 98.47 |
| 2 | 0.36 | 4.52 | 0.90 | 0.02 | 65.55 | 0.10 | 23.01 | 94.45 |
| 3 | 0.08 | 9.44 | 0.05 | 0.02 | 64.38 | 0.17 | 25.83 | 99.71 |
| 4 | 0.05 | 10.96 | 0.12 | 0.08 | 62.87 | 0.03 | 26.51 | 100.11 |
| 5 | 0.07 | 8.23 | 0.05 | 0.05 | 65.90 | 0.05 | 25.41 | 99.66 |
| 6 | 0.82 | 5.53 | | 0.03 | 67.90 | 0.07 | 24.37 | 98.73 |
| 7 | 0.48 | 3.83 | | | 68.94 | | 23.08 | 96.32 |
| 8 | 0.34 | 6.07 | | | 62.27 | | 22.83 | 91.51 |
| 9 | 1.02 | 6.79 | | | 85.05 | | 24.65 | 97.51 |
| 10 | 0.03 | 10.52 | | | 63.01 | | 26.29 | 99.79 |
| 11 | 0.45 | 3.59 | | | 69.08 | | 22.90 | 96.02 |

below. The study was carried out mainly on the samples from the Srednyaya Padma deposit, the largest and the most minutely prospected object in the region.

The study of vanadium-bearing hematite, ore mineral of uranium-vanadium ores, under the raster electron microscope has shown that in all its spectra is a line of vanadium. The content of vanadium does not exceed 1-3% in dispersed hematite and is visibly higher in the compact variety of the mineral, forming isometric aggregations and veinlets. The concentration of vanadium in this hematite fluctuates from 3.59% to 10.96% (Tabl. 1). In polished sections under the microscope, hematite from veinlets and aggregations are represented by the lamellae broken by cracks in longitudinal and transversal directions (Fig. 1). In the cracks more often are clauthalite and carbonate, rarely quartz, clay and other minerals. Under the electron microscope, the lamellar form of hematite aggregations is detected; it is also broken by microcracks on microblocks, in which aggregations of carbonaceous matter with different powdery aggregates often occur, however, in them are no the proper vanadium phases.

The electron microprobe analysis of hematite has shown that the parts of mineral, which are the most enriched by vanadium, look dark grey in back-scattered electrons (Fig. 2); they contain up to 10.98% of vanadium. Significantly less amount of this element (nearly 3-5%) was detected in the hematite lamellae, which look light grey in back-scattered electrons. In reflected light, by measurements of V.A. Rassulov (VIMS) and O.M. Uvarkina (The Fersman Mineralogical Museum), in 15 points noted varieties of hematite are not distinguished. Intensity of reflectance (R) is 25-21% (Fig. 3). Size of unit cell parameters of hematite with increased content of vanadium is following: $a_{rh} = 5.44 \text{ \AA}$, $\alpha = 54^\circ 73'$; $a_{hex} = 5.03$, $c = 13.84 \text{ \AA}$, space group $R\bar{3}c$; in contrast to com-

mon hematite with low content of vanadium (less than 1%), for which unit cell parameters are: $a_{rh} = 5.42 \text{ \AA}$, $\alpha = 55^\circ 17'$; $a_{hex} = 5.04 \text{ \AA}$, $c = 13.76 \text{ \AA}$. By analogy with varieties named titanohematite or aluohematite, for vanadium-enriched hematite one can offer the name vanadiohematite with a formula $(Fe_{1.6-1.9}V_{0.4-0.1})_2O_3$, that was earlier determined (Ryzhev *et al.*, 1991). However, then a distinction of the unit cell parameters of vanadium-bearing and common hematite was not found.

Vanadium-bearing hematite from a fissure zone of oxidation also contains the redeposited uranium and noble metals in high concentrations; they often form powdery aggregates on carbonaceous matter and near it. Among them, the present studies have shown the thin-dispersed aggregations of uranium oxides, isoferroplatinum, Pt_3Fe , native gold, froodite, and auricupride, Cu_3Au . The thin-dispersed well-shaped uranium oxides form the isometric aggregations about $100 \mu m$, sometimes crossed by the hematite microveinlets and microstringers. Moreover, in hematite are the complex uranium iron-vanadium-siliceous compounds. By data of the electron microprobe analyses of single grains, in them, the content of uranium fluctuates from 39.63 to 48.88%; silicon – from 6.73 to 9.79; iron – from 3.62 to 9.96; vanadium – from 4.59 to 4.85; calcium – from 2.26 to 2.56%. In smaller concentrations are the following elements: aluminium – from 0.78 to 1.87; magnesium – from 0.83 to 1.48; sodium – from 0.13 to 0.38; titanium – from 0.08 to 0.18, and phosphorus – from 0.00 to 0.51%. The calculated total of oxides fluctuates from 92.88 to 98.19%. Since the small size of grains, the additional studies of the mineral were not carried out, therefore, its belonging to some mineral species was not determined.

The dendrite aggregations of Pt_3Fe (Fig. 4), 15-3 μm in size, are formed by nanocrystals with a size of 10-15 nm (calculated by data of microd-

Table 2. Calculation of microdiffraction pattern of Pt₃Fe

| Standard data for Pt ₃ Fe (Sel. P. Data, 1974) | | Calculated data for studied sample of Pt ₃ Fe | | <i>hkl</i> |
|--|----------|---|----------|------------|
| <i>d</i> | <i>I</i> | <i>d</i> | <i>I</i> | |
| 3.85 | 25 | 3.90 | 3 | 012 |
| 2.74 | 40 | 2.78 | 5 | 104 |
| 2.22 | 100 | 2.19 | 10 | 110 |
| 1.93 | 90 | 1.82 | 9 | 113 |
| 1.73 | 40 | 1.66 | 5 | 024 |
| 1.57 | 40 | 1.58 | 5 | 116 |
| 1.36 | 90 | | | 214 |
| 1.28 | 25 | 1.25 | 3 | 300 |
| 1.22 | 25 | | | 208 |
| 1.16 | 25 | 1.13 | 3 | 119 |

Table 3. Calculation of microdiffraction pattern of Cu₃Au

| <i>hkl</i> | Standard data for Cu ₃ Au (Bokii, 1954; Garelik <i>et al.</i> , 1970) | | Calculated data for studied sample of Cu ₃ Au | |
|------------|--|----------|--|----------|
| | <i>d</i> | <i>I</i> | <i>d</i> | <i>I</i> |
| 100 | 3.75 | 20 | 3.66 | 3 |
| 110 | 2.65 | 5 | | 9 |
| 111 | 2.17 | 100 | | 10 |
| 200 | 1.88 | 60 | | |
| 210 | 1.67 | 15 | 1.69 | 9 |

Table 4. Calculation of microdiffraction pattern of Cu₃Pd

| <i>hkl</i> | Calculated data | | Standard data (Garelik <i>et al.</i> , 1970) | |
|------------|-----------------|----------|---|-----------|
| | <i>d</i> | <i>I</i> | <i>d</i> | <i>I</i> |
| 110 | 2.57 | 80 | 2.59 | weak |
| 111 | 2.12 | 80 | 2.13 | middle |
| 200 | 1.84 | 100 | 1.84 | strong |
| 210 | 1.64 | 20 | 1.63 | weak |
| 211 | 1.47 | 70 | 1.49 | middle |
| 220 | 1.28 | 80 | 1.30 | middle |
| 300 | 1.20 | 10 | 1.227 | weak |
| 310 | 1.16 | 10 | 1.173 | very weak |
| 311 | 1.08 | 40 | 1.100 | middle |
| 322 | 1.04 | 40 | 1.062 | weak |

iffraction by the Selyakov's equation (Kitaigorodskii, 1952)). Their identification was made on the basis of comparison of microdiffraction pattern of the studied aggregations to standard data (Tabl. 2). Native gold with size of nanocrystals nearly 300-500 nm forms the dendrite aggregates with a size of 800 μm (Fig. 5). The lamellar aggregations of native gold among the prisms of froodite and the small powdery aggregates of gold with a weak microdiffraction pattern were also found (Fig. 6). The size of nanocrystals of auricupride, Cu₃Au, forming the roundish aggregates to 1 μm in size (Fig. 7), is nearly 1-5 nm. Comparison of the microdiffraction patterns of Cu₃Au with standard data is given in Table 3.

Besides auricupride, in hematized dolomite of the bed zone of oxidation, a new mineral phase, the palladium analogue of auricupride, has been found. In the studied sample of dolomite, the carbon-bearing matter was found, which melt under the influence of thermal and radiation electron beam and form the thin films.

The microdiffraction pattern of this film corresponds to the compound Cu₃Pd with a space group Pm₃m and the interplanar distances (Tabl. 4), being characteristic for this compound, $a_0 = 3,68 \pm 0,03 \text{ \AA}$.

A particle (Fig. 8) with a size of 1.5 μm was also found; it was located near a pore in dolomite and overgrown by hematite from the side of this pore, near there was the same particle with size nearly 1.0 μm, overgrown by hematite from every side. The lamellar and hexagonal crystals of palladium analogue of auricupride are marked (Fig. 9). The X-ray characteristic spectra were obtained from a film and several particles of this phase. The results of calculation of quantitative ratios of all presenting chemical elements by four spectra are given in Table 5.

The obtained results show that a ratio of atom amounts of Cu/Pd in them fluctuates from 2.55 to 5.8. At the same time, all studied particles are practically identical by the unit cell parameters in the detection limits. By virtue of that, one can suppose that studied crystals are imperfect, or in them are isomorphous admixtures, which do not significantly influence on the unit cell parameters. Calculated formulae for analysed samples are close to each other. They can be represented as follows: Cu_{3.32}Pd_{0.6} (an. 1); Cu_{3.3}Pd_{0.7} (an. 2, 3); Cu₃Pd_{1.18} (an. 4). The aggregation (an. 2) practically without admixture and the grain (an. 3) containing significant amount of iron and lead have the identical calculated formulae. The differences in measured limits of detection of palladium and copper in the analy-

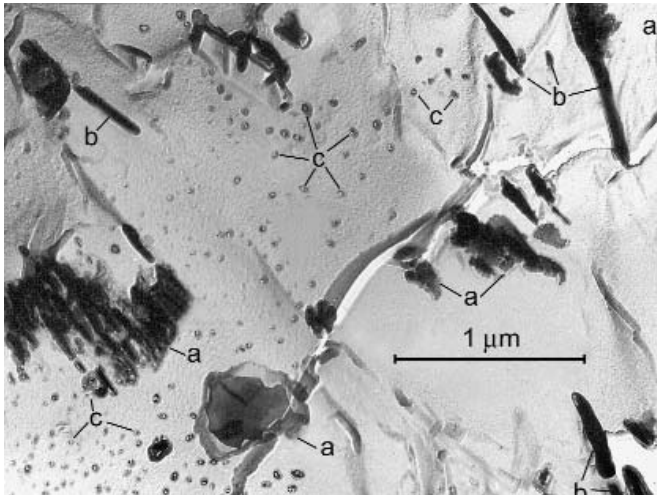


Fig. 6. Lamellar aggregations of native gold (a), prisms of froodite (b). Small powdery aggregates (c) of native gold with weak microdiffraction pattern.

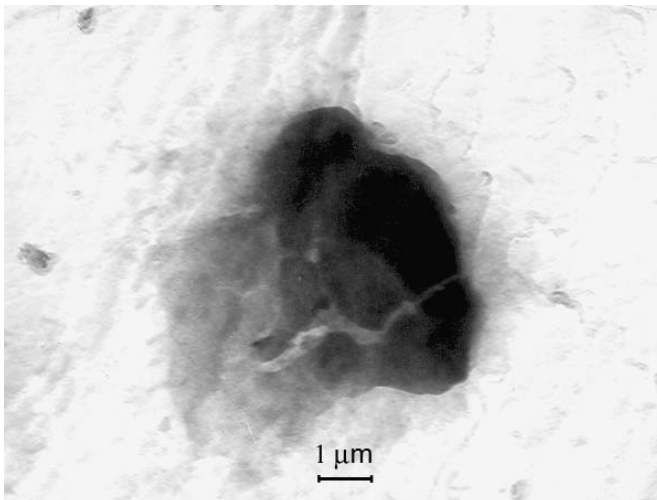


Fig. 7. Roundish aggregates of auricupride broken by cracks.

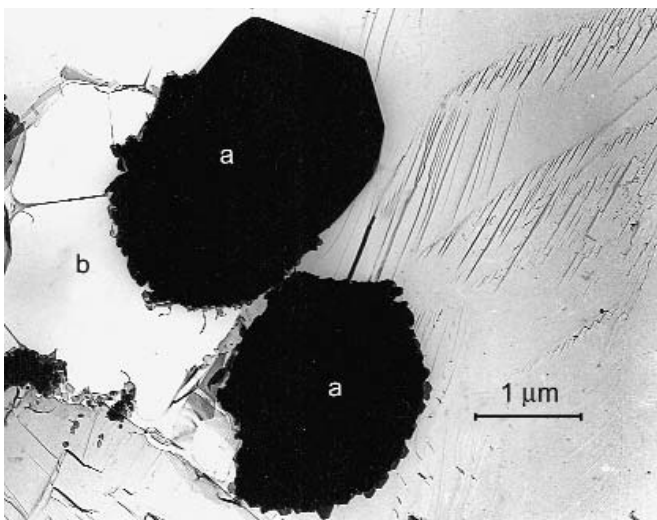


Fig. 8. Aggregations of Cu₃Pd (black, a) near pore (b) in dolomite. Crystal of palladium analogue of auricupride (a) is overgrown by hematite from the side of the pore. The second crystal of palladium analogue of auricupride (a) is overgrown by hematite from every side.

Table 5. Results of calculation of quantitative ratios of chemical elements of palladium analogue of auricupride

| No. | Chemic. E(keV) | Intensity | Content,% | Atom amount, Cu/Pd | |
|-----|----------------|-----------|-----------|--------------------|------|
| 1 | Pd | 2.84 | 217.365 | 12.99 | |
| | Mn | 5.90 | 1.575 | 0.60 | |
| | Fe | 6.40 | 66.198 | 37.12 | 5.8 |
| | Cu | 8.95 | 35.299 | 44.96 | |
| | Pb | 10.55 | 0.342 | 4.32 | |
| 2 | Pd | 2.84 | 192.791 | 26.45 | 4,7 |
| | Cu | 8.05 | 32.860 | 73.55 | |
| 3 | Pd | 2.84 | 245.171 | 14.84 | 4.7 |
| | Fe | 6.40 | 68.352 | 37.48 | |
| | Cu | 8.05 | 36.018 | 41.81 | |
| | Pb | 10.55 | 0.806 | 5.87 | |
| 4 | Pd | 2.84 | 238.087 | 39.70 | 2.55 |
| | Cu | 8.05 | 18.990 | 60.30 | |

Table 6. Interplanar space of intermetal phase CuZn and crystallochemical group of iron

| hkl | Standard data for CuZn (Garelik <i>et al.</i> , 1970) | | Standard data for Fe group. (Mikheev, 1957) | | Расчетные данные CuZn | |
|-----|---|-----------|---|----|-----------------------|----|
| | d | I | d | I | d | I |
| 110 | 2.09 | very weak | 2.02 | 9 | 2.12 | 10 |
| 200 | 1.47 | weak | 1.43 | 7 | 1.50 | 9 |
| 211 | 1.21 | weak | 1.16 | 10 | 1.22 | 5 |
| 220 | 1.04 | middle | 1.02 | 7 | 0.94 | 3 |
| 310 | 0.93 | middle | | | | |
| 222 | 0.85 | middle | | | | |

Table 7. Interplanar space of phase AuO(OH)

| Calculated data | | Standard data (Novgorodova <i>et al.</i> , 1995) | |
|-----------------|---|--|-----|
| d | I | d | hkl |
| 3.45 | 1 | hematite | |
| 2.82 | 4 | hematite | |
| 2.47 | 8 | 2.47 | 111 |
| 2.09 | 9 | 2.02 | 200 |
| 1.72 | 7 | 1.75 | 220 |
| 1.55 | 7 | 1.43 | 311 |

ses 1, 2, and 3, do not also considerably affect on formulae. Consequently, one can admit that analysed samples are represented by imperfect crystals.

In carbonaceous matter, which quite often occurs in hematite, during its study under the raster electron microscope the powdery aggregates of native copper are also observed; they have the increased unit cell parameters that can be connected with a presence of gold in copper. Moreover, on quartz from the hematized dolomite, the powdery aggregates decorating splits were noted; they give the microdiffraction pattern of the iron crystallochemical group and intermetal compound with chemical composition CuZn (Tabl. 6). The size of nanocrystals, used for obtaining of a microdiffraction pattern, is 100-200 nm. The interplanar distances of the CuZn phase are slightly higher than standard ones; that can be connected with a presence of isomorphous iron in this aggregation.

At last, in hematized dolomite, the crushed grain of carbonate mineral was found; it contains an inclusion, on which microdiffraction pattern are the diffusive reflections of the AuO(OH) phase. One failed to measure these reflections earlier; because of that the value «I» in Table 7 in the column «standard data» is absent. The first two lines in the column «calculated data» belong to hematite, with which this phase forms intergrowths; the other four lines belong to the AuO(OH) phase, $a_0 = 4.18 \pm 0.03$ Å. The size of separate particles forming the AuO(OH) grain fluctuates from 100 to 400 nm. The size of nanocrystals is of 100-150 nm.

Conclusion

The studies have shown that dispersed hematite of dolomites from the old deep-seated zone of oxidation, the isometric aggregations and veinlets of lamellar hematite, occurring in the circum-ore space and in uranium-vanadium ores, always contain the increased (more than 1%) concentrations of vanadium. At that, the lamellae of hematite, which look dark grey in back-scattered electrons, are much enriched (in our cases up to 10.96%) by vanadium. It is detected for the first time, that vanadium hematite has the characteristic unit cell parameters distinguishing from the unit cell parameters of hematite with low (less than 1%) concentrations of vanadium.

Vanadium hematite often contains carbonaceous aggregations, on which or near which the redeposited powdery aggregates of gold-bearing copper, auricupride, native gold,

froodite, isoferroplatinum, intermetal compound with chemical composition CuZn, the Fe group and new natural phase of Cu₃Pd type, palladium analogue of auricupride, are noted. The size of nanocrystals of these phases fluctuates from 1-5 nm to 300-500 nm.

In hematized dolomite, a grain of carbonate mineral with diffusive reflections of the AuO(OH) phase was found (the second finding in nature, for the first time definite $a_0 = 4.18 + 0.03 \text{ \AA}$), sizes of its nanocrystals are 100-150 nm.

The presence of carbonaceous matter with powdery aggregates of nanocrystals of gold-bearing native copper, auricupride, intermetal compounds of CuZn type, crystallochemical group of iron, Pt₃Fe, Cu₃Pd in hematite is important for the working of technological processes of extraction of noble metals from ores, understanding of their genesis and reasons of frequent discrepancy in analytical data on noble metals. The joint occurrence of carbonaceous matter and noble metals and also other intermetal compounds is an evident that in process of their transportation and sedimentation the carbonaceous matter played a significant, unless decisive, role. The separation of noble metals on carbonaceous matter and near it is also an evident that analytical data on content of noble metals in ores and in the zone of hematization of rocks can be understated since during analysis process they evaporate together with carbon. Therefore, the previous forecasts (Chernikov, 1997, 2001, Chernikov *et al.*, 2000) about large reserves of noble metals in the region of the Onezhskaya depression have one more indirect confirmation.

References

- Bokii G.B.* Introduction in Crystallochemistry. (Vvedenie v Kristallokhimiyu). M.: MGU. **1954**. 482 p. (Rus.).
- Chernikov A.A.* Correlation of processes of the weathering crust and hypogenic factors during formation of the complex (V, Pd, Pt, Au, U) deposits of Onezhskii type "In book: Glavnye Geologicheskie i Kommercheskie Tipy Mestorozhdenii Kor Vyvetrivaniya i Rossypei, Tekhnologicheskaya Otsenka i Razvedka. M.: IGEM RAN. **1997**. P. 117. (Rus.).
- Chernikov A.A.* Deep-seated Hypergenesis, Mineral and Ore Formation. (Glubinnyi Gipergenez, Mineralo- i Rudoobrazovanie). M.: Min. Musei im. A.E. Fersmana RAN. **2001**. 100 p. (Rus.).
- Chernikov A.A., Khitrov V.G., Belousov G.E.* Role of carbonaceous matter in formation of the large polygenic complex deposits of the Onezhskii type "In book: Uglerodso-derzhashchie Formatsii v Geologicheskoi Istorii. Petrozavodsk: KNTs RAN. **2000**. P. 194-199. (Rus.).
- Garelik S.S., Rastorguev L.N., Skakov Yu.A.* X-Ray Diffraction Electron Optic Analysis. (Rentgenograficheskii Elektronnooptiches-kii Analiz). M.: Metallurgiya. **1970**. 36 p. (Rus.).
- Kitaigorodskii A.I.* X-Ray Structural Analysis of Microcrystal and Amorphous Bodies. (Rentgenostrukturnyi Analiz Melkokristallicheskih i Amorfnykh Tel). M.: Gos. Isd. Tekhn.-Teor. Lit. **1952**. 586 p. (Rus.).
- Mikheev V.I.* X-Ray Determiner of Minerals. (Rentgenovskii Opredelitel' Mineralov). M.: Gosgeolizdat. **1957**. 820 p. (Rus.).
- Novgorodova M.I., Trubkin N.V., Generalov M.E.* New gold in crusts of weathering of the South Ural (Russia) "Dokl. RAN. **1995**. V. 344. N. 4. P. 525-529. (Rus.).
- Poluektov V.V., Chernikov A.A., Ryzhov B.I.* Peculiarities of formation of mineral assemblages of the large complex (V, Pd, Pt, Au, U) deposits of the Onezhskii depression of the Baltiiskii shield " In book: Krupnye i Unikal'nye Mestorozhdeniya Redkikh i Blagorodnykh Metallov. SPb.: SPb. Gornyi Institut im. G.V. Plekhanova. **1998**. P. 240-246. (Rus.).
- Ryzhov B.I., Troneva N.V., Polekhovskii Yu.S.* Vanadium hematites in metasomatites of Zaonezh'e (Kareliya) " Izv. AN SSSR. Ser. geol. **1991**. N. 10. P. 133-139. (Rus.).
- Selected Powder Data for Mineral (first edi-

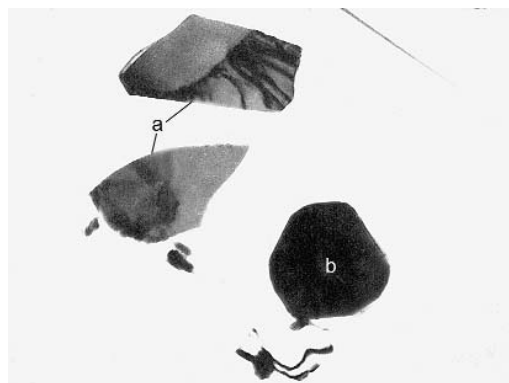


Fig. 9. Lamellar (a) and hexagonal (b) aggregations of Cu₃Pd